Building Effective Representations for Sketch Recognition

Jun Guo
Sun Yat-sen University,
Guangzhou, P.R.China

Changhu Wang
Microsoft Research,
Beijing, P.R.China

Hongyang Chao
Sun Yat-sen University,
Guangzhou, P.R.China

Abstract

As the popularity of touch-screen devices, understanding a user's hand-drawn sketch has become an increasingly important research topic in artificial intelligence and computer vision. However, different from natural images, the hand-drawn sketches are often highly abstract, with sparse visual information and large intra-class variance, making the problem more challenging. In this work, we study how to build effective representations for sketch recognition. First, to capture saliency patterns of different scales and spatial arrangements, a Gabor-based low-level representation is proposed. Then, based on this representation, to discovery more complex patterns in a sketch, a Hybrid Multilayer Sparse Coding (HMSC) model is proposed to learn mid-level representations. An improved dictionary learning algorithm is also leveraged in HMSC to reduce overfitting to common but trivial patterns. Extensive experiments show that the proposed representations are highly discriminative and lead to large improvements over the state of the arts.

Introduction

Sketching is a natural way for users to record, express, and communicate. Compared with texts, it provides a more expressive way to render users' rough ideas via natural drawing. Thus, in the era of touch screens, how a computer can recognize a user's hand-drawn sketch, as a basic problem in artificial intelligence, has attracted more and more attentions.

Although sketch recognition has been studied for more than twenty years, most of existing work was limited to some narrow domains, such as chemical drawings (Ouyang and Davis 2011), diagrams (Peterson et al. 2010), or simple hand-drawn shapes such as circles and rectangles (Paulson and Hammond 2008; Jie et al. 2014). In recent years, some algorithms (Eitz, Hays, and Alexa 2012; Sun et al. 2012) were developed to recognize sketches of general objects without any domain knowledge, as shown in Fig. 1. We will also focus on recognizing general sketches in this work.

Different from natural images, the hand-drawn sketches are often highly abstract and lack of color and textures. Thus, existing algorithms for natural images cannot be directly applied to this problem. The sparsity of visual information and complexity of internal structures make the problem more challenging. In fact, even humans can only achieve a recognition accuracy of 73.1% (Eitz, Hays, and Alexa 2012).

Figure 1: Examples of hand-drawn sketches.

Some prior research on sketch-based retrieval favors non-vector-based representations. (Cao et al. 2011) and (Sun et al. 2012) employed a global sketch matching approach to measure similarity between two sketches via the improved Chamfer distance, and proved to work well in web-scale databases. However, such methods are more appropriate for retrieval rather than recognition, since lots of widely-used classifiers require vector-based input. On the other hand, existing vector-based representations on sketch recognition usually rely on dense sampling and large local patches to deal with the sparsity problem in sketches. (Eitz et al. 2011) provided a detailed comparison of these representations including Shape Context (Belongie, Malik, and Puzicha 2002), Histogram of Oriented Gradients (Dalal and Triggs 2005) and their variants. The comparison result showed that HOG-like representations by summing up gradients of strokes in a grid generally outperform others in sketch-related tasks. (Hu and Collomosse 2013) also conducted experiments on SIFT (Lowe 2004) and Self Similarities (Shechtman and Irani 2007), and obtained consistent results. Based on these conclusions, (Eitz, Hays, and Alexa 2012) designed robust gradient-based visual descriptors to form a low-level representation, and fed them into the Bag-of-Words (BoW) framework with soft assignment (van Gemert et al. 2008) to build a mid-level representa-

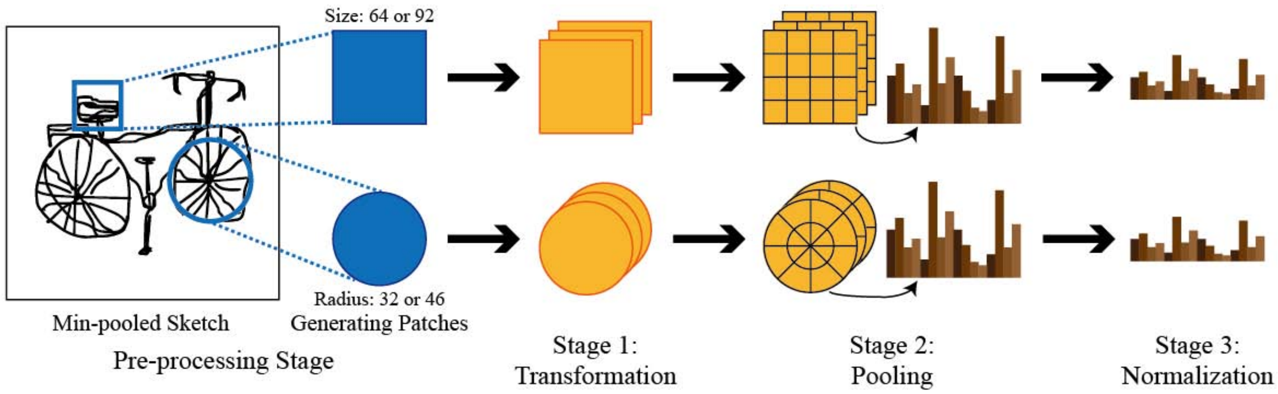

Figure 2: Processing stages for building our local descriptors. For a clearer view, we don't show the min-pooling step of the pre-processing stage. That is, the initial input of the shown pipeline is a min-pooled sketch image.

tion, which achieved the state-of-the-art performance. Jayasumana (Jayasumana et al. 2014) got slightly better results by using an improved Kernel SVM classifier, keeping the representations unchanged.

In spite of the success of Eitz's representation (Eitz, Hays, and Alexa 2012), there are still two main problems to restrict its performance. First, its visual descriptors are built upon fixed-size patches, with each patch uniformly divided into square cells. Such neglect in scales and spatial arrangements of local patterns cannot be compensated in higher-level representations, and thus limit the discriminability of the whole model. The other disadvantage is from the over-simplified mid-level representation. The BoW framework employed by Eitz *et al*. used simple k-means algorithm to learn the mid-level representation, which is far from enough to further discover abstract and discriminative patterns.

To overcome these two problems, in this paper, we propose a novel model to represent hand-drawn sketches, including a Gabor-based low-level representation followed by a sophisticated mid-level representation named Hybrid Multilayer Sparse Coding (HMSC). To solve the first problem, in the low-level representation we first pre-processes the input sketch to reduce scale and translation variances. Then patches of multiple sizes are extracted and Gabor transforms are applied to decouple stroke orientations. Furthermore, multiple pooling strategies are exploited to produce descriptors varying in scales and spatial arrangements, which are further normalized and fed into HMSC. In order to fully take use of these descriptors and discover more abstract and discriminative sketch patterns, so as to solve the second problem, the HMSC representation is constructed with sparse coding as the basic building block. First, in each Multilayer Sparse Coding (MSC) model, input features are processed through multiple layers of convolutional sparse coding, pooling and normalization sequentially. Then, multiple MSC models with different input descriptor types are merged to result in the HMSC model, which encodes descriptors of various scales and spatial arrangements separately, and combines outputs from various layers. Moreover, a mutual incoherence constraint is introduced to HMSC to avoid overfitting to trivial patterns with little discriminability. Based on the proposed representations, the recognition accuracy on the benchmark dataset is improved to 68.5% from the state-of-the-art 57.9%.

Building Local Descriptors

The proposed low-level representation represents a sketch by local descriptors. There are three processing stages to build such a descriptor. The initial input is a local patch of the sketch and the final output is a vector of N dimensions. Before these three stages, a pre-processing stage for generating local patches is also involved. The whole pipeline is shown in Fig. 2. We now describe each stage sequentially.

Pre-processing Stage

Each sketch image (zero pixel value for strokes and ones for background) is rescaled via min pooling to guarantee that the longer side is 224 pixels. Then, it is put in the center of a blank image with an area of 256×256 to produce a blank border with at least 16-pixel width. Such borders can reduce the boundary effect that may occur during the execution of some operations like filtering.

After that, sketch patches are extracted at points generated by uniformly dense sampling on sketch images. To discover patterns of different scales, multiple types of patches are extracted. In this work, we sample 32×32 points and utilize square patches with sizes of 64 and 92 plus circular patches with radii of 32 and 46.

Stage 1: Transformation

The transformation stage maps a local patch to multiple channels, each of which has the same resolution as the input patch. More precisely, we apply real Gabor filters at each patch pixels using R orientations and compute the magnitude response to generate R response channels. Note that the wavelength of a real Gabor filter should not be too large compared with its scale, so that the filter can provide narrow orientation tuning. We have tried filters which give broader orientation tuning, e.g., Eitz's Gaussian's first order derivative (Eitz, Hays, and Alexa 2012), but observed worse per-

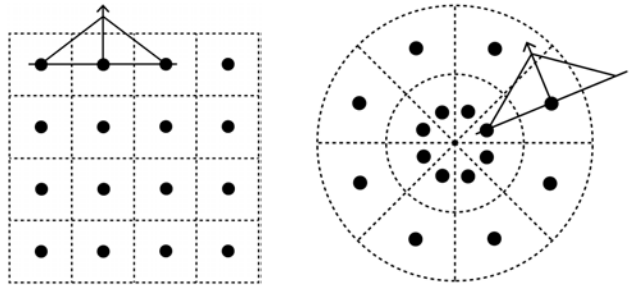

(a) A 4×4 square grid with bilinear weights

(b) A 2×8 polar grid with bilinear weights

Figure 3: Two different pooling strategies used in our work. Black spots in the image represent pooling centers.

formance. This might because that sketch patches are composed of thin strokes, so that filters with narrow orientation tuning can better decouple multiple orientations at each pixel, especially near the junctions of strokes.

In this work R is set to 9. The other parameters of Gabor filters, i.e., the scale, the wavelength of the sinusoidal factor, and the spatial aspect ratio are set to $5, 9, 1$ respectively.

Stage 2: Pooling

Given R channels, the pooling stage spatially accumulates pixel values in each channel, so that each channel is transformed into a vector of length C. All R resulting vectors are concatenated to form a unnormalized descriptor of $R \times C$ dimensions. Two pooling strategies are applied, hoping to capture patterns of different spatial arrangements.

[Square Grid] We use a 4×4 square grid of pooling centers (Fig. 3(a)). Pixel values within a *square* channel are summed spatially by bilinearly weighting them according to their distances from the pooling centers. That is, the output for each channel is a $(C = 16)$-dimension histogram consisting of 4×4 spatial bins.

[Polar Grid] A polar arrangement is adopted (Fig. 3(b)). A *circular* channel is first divided into 2 distance intervals and further uniformly split into 8 polar sectors. Then a histogram of $(C = 8 \times 2)$ dimensions is generated by summing up pixel values bilinearly weighted in polar coordinates. Besides, inspired by (Roman-Rangel et al. 2011), distance intervals are $L2$-normalized independently to balance their contributions when building histograms.

Stage 3: Normalization

The unnormalized descriptors from the previous stage are combinations of histograms generated by summing up pixel values, whose magnitudes vary over a wide range due to the variations in stroke length. Thus, an effective normalization is needed to improve the performance. We experimented with $L1$-norm and $L2$-norm normalizations, and found that the latter was consistently better. Therefor, a descriptor $\bar{\mathbf{x}}$ from the previous stage is normalized by:

$$\mathbf{x} = \frac{\bar{\mathbf{x}}}{\sqrt{\|\bar{\mathbf{x}}\|_2^2 + \epsilon}}, \tag{1}$$

where ϵ is a small positive number.

Hybrid Multilayer Sparse Coding (HMSC)

In this section we introduce the proposed mid-level representation, i.e., the Hybrid Multilayer Sparse Coding (HMSC) model. First, the standard sparse coding algorithm is briefly introduced, which is the building block of the HMSC model. Then, an improved dictionary learning algorithm is presented to avoid overfitting to trivial sketch patterns. Finally, we discuss how to build the mid-level representation via the improved sparse coding algorithm in a hybrid and multilayer manner.

Standard Sparse Coding

We need a more powerful model to encode the proposed local descriptors to a mid-level representation. Sparse coding is adopted here as a building block of HMSC, since existing research has shown its encouraging performance compared with other encoding schemes like BoW (Boureau et al. 2010). It tries to reconstruct all inputs using parsimonious representations, the sparsity constraint of which makes it possible to discover salient patterns that are hard to be manually explored and thus improve the discriminability. We first briefly introduce the standard sparse coding in this section.

Let $\mathbf{X}$ be M local descriptors in an N-dimension vector space, i.e. $\mathbf{X} = [\mathbf{x}_1, \ldots, \mathbf{x}_M] \in \mathbb{R}^{N \times M}$. The key idea of sparse coding is to represent vectors in $\mathbf{X}$ as linear combinations of codewords taken from a learned dictionary $\mathbf{D} = [\mathbf{d}_1, \ldots, \mathbf{d}_K] \in \mathbb{R}^{N \times K}$ with sparse constraint. It can be formulated as a matrix factorization problem with an $L1$-norm penalty:

$$\begin{aligned} &\min_{\mathbf{D},\mathbf{Y}} \sum_{m=1}^{M} \|\mathbf{x}_m - \mathbf{D}\mathbf{y}_m\|_2^2 + \lambda \|\mathbf{y}_m\|_1, \\ &\text{s.t.} \quad \|\mathbf{d}_k\|_2 \leq 1, \quad \forall k = 1, 2, \ldots, K, \end{aligned} \tag{2}$$

where $Y = [\mathbf{y}_1, \ldots, \mathbf{y}_M] \in \mathbb{R}^{K \times M}$ is a matrix containing the associated sparse combinations (a.k.a. sparse codes), and λ is the sparsity level.

The above optimization problem is convex for $\mathbf{D}$ (with $\mathbf{Y}$ fixed) and $\mathbf{Y}$ (with $\mathbf{D}$ fixed) respectively, which can be solved by alternatively optimizing $\mathbf{D}$ and $\mathbf{Y}$ (Lee et al. 2006).

Improved Dictionary Learning

Since sketch images are visually sparse and only consist of several strokes, most local patches of sketches belong to some simple but trivial patterns, e.g., a horizontal line, a right angle, and so forth. Complex but discriminative patterns, such as a face which strongly suggests the existence of a human-like sketched object, are infrequently observed. Considering that the initial inputs of the sparse coding algorithm are descriptors extracted from local patches, the learned dictionary might overfit to those frequent but unimportant patterns. To promote importance of less frequently observed patterns so as to enrich codewords, we try to learn a dictionary within which codewords are of highly mutual incoherence. This idea is inspired by parts of works like

(Tropp 2004), (Daubechies, Defrise, and De Mol 2004), (Elad 2007) and (Eldar and Mishali 2009) which showed that both the speed and accuracy of sparse coding depend on the incoherence between codewords.

To achieve the above goal, we add a mutual incoherence constraint in the standard sparse coding algorithm:

$$\begin{aligned}
&\min_{\mathbf{D},\mathbf{Y}} \sum_{m=1}^{M} \|\mathbf{x}_m - \mathbf{D}\mathbf{y}_m\|_2^2 + \lambda \|\mathbf{y}_m\|_1, \\
&\text{s.t.} \quad \|\mathbf{d}_k\|_2 \leq 1, \quad \forall k = 1, 2, \ldots, K, \\
&\qquad \|\mathbf{d}_i^T \mathbf{d}_j\|_1 < \eta, \quad \forall i, j = 1, 2, \ldots, K, i \neq j,
\end{aligned} \tag{3}$$

where η is the mutual incoherence threshold. This optimization objective is somewhat similar to (Ramirez, Sprechmann, and Sapiro 2010), (Barchiesi and Plumbley 2013) and (Bo, Ren, and Fox 2013), but the first one tried to promote mutual incoherence of dictionaries rather than codewords via an $L2$-norm penalty. The latter two ones focused on accuracy optimization algorithms. To accelerate the optimization process they required an $L0$-norm sparsity constraint to strictly limit the number of nonzero elements, and thus are not suitable here.

For efficiency, here we introduce an approximate algorithm to solve Eq. (3). We keep the learning phase and the coding phase unchanged, but plug in a dictionary sweeping phase between them.

More detailedly, in each iteration, after the learning phase we sequentially scan each learned codeword. For a codeword $\mathbf{d}_i$, if there exists another codeword $\mathbf{d}_j (j > i)$ having $\|\mathbf{d}_i^T \mathbf{d}_j\|_1 \geq \eta$, i.e., violating the mutual incoherence constraint, $\mathbf{d}_i$ will be marked as obsolete. At the end of scanning, the swept dictionary may be composed of less than K valid codewords and thus requires a supplement. In this case, we simply go back to the input dataset $\mathbf{X}$, sample some vectors from it, multiply their corresponding sparse codes and the current dictionary so as to obtain their sparse approximations, and then compute the approximation errors. Sampled vectors with highest errors imply high independence of the current codewords. Thus, we replace obsolete codewords with these vectors. And the coding phase follows.

This simple algorithm proves to work very well according to experiments.

Multilayer Sparse Coding (MSC)

In this section we introduce the Multilayer Sparse Coding (MSC) model, a simplified version of our HMSC. We will introduce the architechture of HMSC in the next section.

MSC builds a representation layer by layer, with each layer consisting of two stages. In the first layer, the input is a set of local descriptors built upon one type of patch (e.g., square patches with an area of 64^2). In a higher layer, the input is a set of pooled-and-normalized codes from its previous layer. We now describe each stage sequentially.

[Stage 1: Convolutional Sparse Coding] To consider the spatial information and also to achieve local translation invariance, we perform convolutional coding. Given $H \times W$ input vectors of N dimensions belonging to a sketch, every $h \times w$ adjacent vectors are concatenated in order to produce $(H - h + 1) \times (W - w + 1)$ vectors of hwN dimensions. These hwN-dimension vectors are then sparsely encoded, while the dictionary is learned over sketches with a mutual incoherence constraint (as discussed in the previous section).

[Stage 2: Pooling and Normalization] To further achieve the property of translation-invariance and also reduce data size, spatial max pooling is applied to aggregate sparse codes from the previous stage.

For $H \times W$ sparse codes generated by Stage 1 of all layers except the final one, they are spatially divided into groups of $h \times w$ vectors with an overlap ratio of 0.5[1]. Codes within each group are max-pooled, resulting in $\left\lfloor \frac{H-h}{h/2} + 1 \right\rfloor \times \left\lfloor \frac{W-w}{w/2} + 1 \right\rfloor$ pooled codes.

For sparse codes coming from Stage 1 of the final layer, Spatial Pyramid Pooling (Lazebnik, Schmid, and Ponce 2006) is applied.

Pooled codes are then $L2$-norm normalized individually. We have experimented with $L1$-norm normalization but did not observe better results.

Architecture of HMSC

A single MSC has the ability of learning mid-level representations in an unsupervised way. What's more, by spatial pooling, the learned representations achieve the property of local translation invariance and are very stable. However, it only builds on one type of sketch patch, which limits its power to discover patterns of different scales and spatial arrangements. Besides, although outputs produced by the highest layers are robust and abstract, they miss some local details which may be useful to distinguish highly similar sketch categories like armchair and chair. Therefore, the proposed Hybrid Multilayer Sparse Coding (HMSC) model further organizes multiple MSCs in a hybrid way, hoping to exploit the advantages of MSC with its limitations reduced. The whole pipeline of HMSC is shown in Fig. 4.

Generally speaking, HMSC encodes patches of various scales and spatial arrangements, and combines outputs from various layers. First, four types of patches, i.e., square patches with an area of 64^2 and 92^2, circular patches with an area of $32^2\pi$ and $46^2\pi$, are generated, from which descriptors are extracted. Descriptors from different types of patches go through different one-layer MSCs and the outputs (named as S1.1, S1.2, C1.1 and C1.2 respectively) are concatenated. To improve robustness to local deformations and capture more abstract patterns, two-layer MSCs are also exploited. Considering that the input for the second layer has dropped lots of local details, to better render local structures, instead of building four two-layer MSCs individually, pooled codes belonging to 64×64 and 92×92 square patches are merged to be the input of the second layer. Similarly, pooled codes related to circular patches are concatenated and fed into the second layer. Outputs from these two

[1]For an easy explanation, we again use H, W, h and w to represent the number of input vectors and the number of adjacent vectors. We hope this slight overuse does not bring any ambiguity.

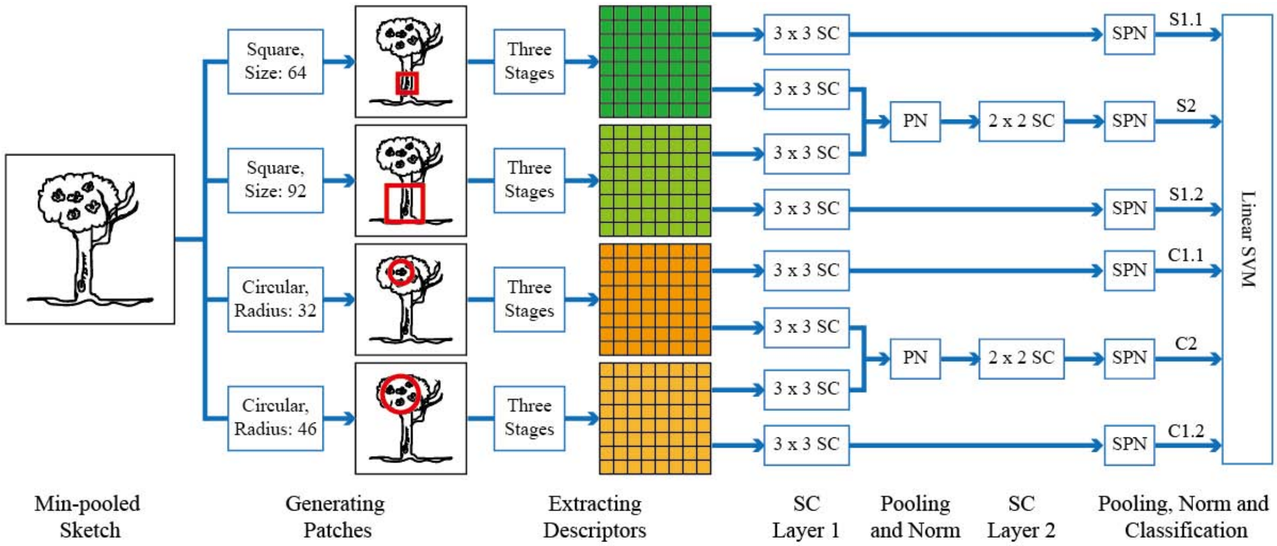

Figure 4: Architecture of HMSC. Sketch patches of different types (including 64×64 / 92×92 square patches and $32 \times 32 \times \pi$ / $46 \times 46 \times \pi$ circular patches) are generated from a min-pooled sketch and then encoded as local descriptors. These descriptors are further fed into multiple layers of convolutional sparse coding (indicated as SC), with a pooling-and-normalization operation (indicated as PN) inserted between SC layers. All sparse codes are finally transformed by a spatial-pyramid-pooling-and-normalization operation (indicated as SPN), and then concatenated to build the final representation, which is classified by a linear SVM. For a clearer view, we only show 8×8 descriptors for the sketch.

two-layer MSCs (named as S2 and C2 individually) are also combined with those from one-layer MSCs.

In our work, all one-layer MSCs learn dictionaries of 2000 codewords. For a two-layer MSC, the first layer learns a 1000-codeword dictionary and its output is max-pooled with the group size of 4×4, followed by the $L2$-norm normalization. Then comes the second layer which learns a dictionary of 2000 codewords. The final stage of each MSC applies a three-level Spatial Pyramid Max-Pooling with each level generating 1×1, 2×2 and 3×3 pooled codes respectively. Note that although the final (concatenated) outputs are indeed vectors of a high dimension, owning to the sparsity they only require a small amount of memory and operating them is usually efficient. We use the Liblinear package (Fan et al. 2008) to learn a linear SVM for classification.

Hyper-parameters not mentioned, e.g. λ and η of sparse coding, are automatically chosen via cross-validation.

Experiments

In this section, we evaluate the proposed representations on the largest sketch dataset collected by Eitz (Eitz, Hays, and Alexa 2012), which contains $20,000$ sketches in 250 categories. This dataset is quite challenging as sketches in each category are very diverse. Even humans can only achieve a recognition rate of 73.1%. Following Eitz's evaluation protocol, we partition the dataset into three parts and perform three-fold cross-test: each time two parts are used for training and the remaining part for testing. The mean classification accuracy of three folds is reported.

Table 1: Mean classification accuracy and learning time of different encoding schemes. Experiments were performed on a laptop equipped with an Intel Core i7. BoW-Soft: Bag-of-Words with soft assignment; SC-Std: standard sparse coding; SC-Const: sparse coding with an $L1$-norm mutual incoherence constraint, i.e., our approach.

Algorithm	Mean Accuracy	Learning Time
BoW-Soft	58.2%	18 min
SC-Std	61.7%	30 min
SC-Const	64.6%	32 min

Mutual Incoherence Constraint & Low-level Representation

We investigated the effectiveness of the added mutual incoherence constraint on a one-layer MSC (including a 3×3 convolutional sparse coding operation, a spatial pyramid max-pooling operation, and a normalization operation) in terms of classification accuracy and learning time. We learned a 2000-codeword dictionary on descriptors built upon 64×64 square patches. To reduce experiment time, we only sampled $1,000,000$ descriptors for learning (no significant improvement was observed when using all descriptors). As a baseline, we also encoded the proposed low-level representations using BoW with soft assignment (BoW-Soft) (van Gemert et al. 2008). The results are shown in Table 1.

[Dictionary Learning] We can see that, standard sparse coding performed much better than Bag-of-Words (BoW) with an acceptable time overhead, consistent with existing

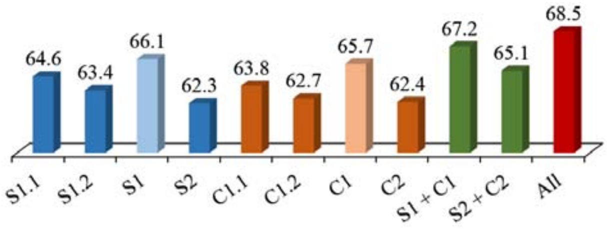

Figure 5: Classification accuracy of components of HMSC. For the definition of S1.1, S1.2, S2, C1.1, C1.2 and C2, please refer to previous sections and Fig. 4. Here we introduce several new symbols. S1: the combination of S1.1 and S1.2; S1 + C1: the combination of S1 and C1; C1 and S2 + C2 are defined similarly to S1 and S1 + C1 respectively; All: S1 + C1 + S2 + C2.

research. What's more, it greatly outperformed Eitz's model (56.0%). Moreover, with the mutual incoherence constraint, sparse coding achieved higher accuracy with comparable learning time, verifying the effectiveness of learning a rich dictionary with diverse codewords.

[Low-level Representation] Notice that here we adopted a simplified version (single scale, single spatial arrangement) of our low-level representation. Nevertheless, directly applying BoW on it has exceeded Eitz's reported accuracy (which also used BoW), indicating the effectiveness of our low-level representation.

The rest experiments are based on the improved sparse coding algorithm.

Mid-Level Representation

To verify the effectiveness of components of HMSC, we list the recognition rate of each component in Fig. 5.

[Scale] By concatenating the outputs of S1.1 and S1.2, S1 performed better than both of them. Compared with C1.1 or C1.2, C1 also brought large improvement. These two comparison results indicate that, by learning representations at multiple scales, we can capture different nontrivial patterns, resulting in performance improvement.

[Spatial Arrangement] Similarly, higher accuracy can be obtained after merging the outputs of S1 and C1, or merging the outputs of S2 and C2. This shows that representations built on various spatial arrangements are complementary and can discover more discriminative patterns.

[Layer] Now we further investigate the effect of layers of HMSC. As shown in Fig. 5, four one-layer MSCs (S1.1, S1.2, C1.1, C1.2) performed surprisingly well, all of which outperformed the state of the arts. Although the two-layer MSCs (S2, C2) performed worse than one-layer ones, merging all MSCs (S1, S2, C1, C2) achieved the highest accuracy of 68.5%. This result confirms that outputs from different layers are good at modeling sketch structures at different level of abstraction, and they can work together to make up a better model.

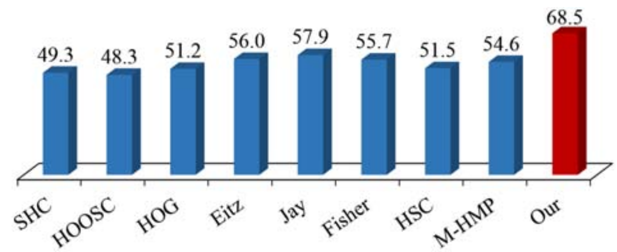

Figure 6: Classification accuracy on the benchmark dataset. SHC: shape context (Belongie, Malik, and Puzicha 2002); HOOSC: histogram of orientation shape context (Roman-Rangel et al. 2011); HOG: histogram of oriented gradient (Dalal and Triggs 2005); Eitz: Eitz's model (Eitz, Hays, and Alexa 2012), Jay: Jayasumana's improved model (Jayasumana et al. 2014); Fisher: Fisher kernel (Perronnin, Sánchez, and Mensink 2010); HSC: Hierarchical Sparse Coding (Yu, Lin, and Lafferty 2011); M-HMP: Multipath Hierarchical Matching Pursuit (Bo, Ren, and Fox 2013).

In short, the above three subsections have verified the usefulness of building representations at various scales, spatial arrangements, and layers.

Compared with State of the Arts

To the best of our knowledge, the state of the arts in sketch recognition on this benchmark dataset achieved the accuracies of 56.0% (Eitz, Hays, and Alexa 2012) and 57.9% (Jayasumana et al. 2014). We also implemented some typical works in natural image recognition and shape analysis (see Fig. 6), but did not observe better results.

As shown in Fig. 6, the performance of our proposed model (68.5%) greatly outperformed the state of the arts. It should be noted that, both Eitz's and Jayasumana's works used a Kernel SVM for classification, while we applied a linear one. By carefully selecting a more effective classifier, our model has potential to reach a higher recognition rate. In addition, recalling that humans can only reach an accuracy of 73.1% on this dataset, our result is quite promising.

Conclusion

In this paper, we systematically studied how to build effective representations for sketch recognition. We designed a Gabor-based low-level representation, based on which a mid-level representation named Hybrid Multilayer Sparse Coding was proposed. By learning sparse codes with an additional constraint on various scales and spatial arrangements, and performing encoding through a varying number of layers, the proposed representations achieved a promising accuracy 68.5% (human's accuracy being 73.1%), leading to a large improvement over the state of arts 57.9%.

Acknowledgments

This work was partially supported by NSF of China under Grant 61173081 and Guangdong Natural Science Foundation, P.R.China, under Grant S2011020001215.

References

Barchiesi, D., and Plumbley, M. D. 2013. Learning incoherent dictionaries for sparse approximation using iterative projections and rotations. *Signal Processing, IEEE Transactions on* 61(8):2055–2065.

Belongie, S.; Malik, J.; and Puzicha, J. 2002. Shape matching and object recognition using shape contexts. *Pattern Analysis and Machine Intelligence, IEEE Transactions on* 24(4):509–522.

Bo, L.; Ren, X.; and Fox, D. 2013. Multipath sparse coding using hierarchical matching pursuit. In *Computer Vision and Pattern Recognition (CVPR), 2013 IEEE Conference on*, 660–667. IEEE.

Boureau, Y.-L.; Bach, F.; LeCun, Y.; and Ponce, J. 2010. Learning mid-level features for recognition. In *Computer Vision and Pattern Recognition (CVPR), 2010 IEEE Conference on*, 2559–2566. IEEE.

Cao, Y.; Wang, C.; Zhang, L.; and Zhang, L. 2011. Edgel index for large-scale sketch-based image search. In *Computer Vision and Pattern Recognition (CVPR), 2011 IEEE Conference on*, 761–768. IEEE.

Dalal, N., and Triggs, B. 2005. Histograms of oriented gradients for human detection. In *Computer Vision and Pattern Recognition, 2005. CVPR 2005. IEEE Computer Society Conference on*, volume 1, 886–893. IEEE.

Daubechies, I.; Defrise, M.; and De Mol, C. 2004. An iterative thresholding algorithm for linear inverse problems with a sparsity constraint. *Communications on pure and applied mathematics* 57(11):1413–1457.

Eitz, M.; Hildebrand, K.; Boubekeur, T.; and Alexa, M. 2011. Sketch-based image retrieval: Benchmark and bag-of-features descriptors. *Visualization and Computer Graphics, IEEE Transactions on* 17(11):1624–1636.

Eitz, M.; Hays, J.; and Alexa, M. 2012. How do humans sketch objects? *ACM Trans. Graph.* 31(4):44.

Elad, M. 2007. Optimized projections for compressed sensing. *Signal Processing, IEEE Transactions on* 55(12):5695–5702.

Eldar, Y. C., and Mishali, M. 2009. Robust recovery of signals from a structured union of subspaces. *Information Theory, IEEE Transactions on* 55(11):5302–5316.

Fan, R.-E.; Chang, K.-W.; Hsieh, C.-J.; Wang, X.-R.; and Lin, C.-J. 2008. Liblinear: A library for large linear classification. *The Journal of Machine Learning Research* 9:1871–1874.

Hu, R., and Collomosse, J. 2013. A performance evaluation of gradient field hog descriptor for sketch based image retrieval. *Computer Vision and Image Understanding* 117(7):790–806.

Jayasumana, S.; Hartley, R.; Salzmann, M.; Li, H.; and Harandi, M. 2014. Optimizing over radial kernels on compact manifolds.

Jie, W.; Changhu, W.; Liqing, Z.; and Yong, R. 2014. Sketch recognition with natural correction and editing. In *AAAI*.

Lazebnik, S.; Schmid, C.; and Ponce, J. 2006. Beyond bags of features: Spatial pyramid matching for recognizing natural scene categories. In *Computer Vision and Pattern Recognition, 2006 IEEE Computer Society Conference on*, volume 2, 2169–2178. IEEE.

Lee, H.; Battle, A.; Raina, R.; and Ng, A. Y. 2006. Efficient sparse coding algorithms. In *Advances in neural information processing systems*, 801–808.

Lowe, D. G. 2004. Distinctive image features from scale-invariant keypoints. *International journal of computer vision* 60(2):91–110.

Ouyang, T. Y., and Davis, R. 2011. Chemink: a natural real-time recognition system for chemical drawings. In *Proceedings of the 16th international conference on Intelligent user interfaces*, 267–276. ACM.

Paulson, B., and Hammond, T. 2008. Paleosketch: accurate primitive sketch recognition and beautification. In *Proceedings of the 13th international conference on Intelligent user interfaces*, 1–10. ACM.

Perronnin, F.; Sánchez, J.; and Mensink, T. 2010. Improving the fisher kernel for large-scale image classification. In *Computer Vision–ECCV 2010*. Springer. 143–156.

Peterson, E. J.; Stahovich, T. F.; Doi, E.; and Alvarado, C. 2010. Grouping strokes into shapes in hand-drawn diagrams. In *AAAI*, volume 10, 14.

Ramirez, I.; Sprechmann, P.; and Sapiro, G. 2010. Classification and clustering via dictionary learning with structured incoherence and shared features. In *Computer Vision and Pattern Recognition (CVPR), 2010 IEEE Conference on*, 3501–3508. IEEE.

Roman-Rangel, E.; Pallan, C.; Odobez, J.-M.; and Gatica-Perez, D. 2011. Analyzing ancient maya glyph collections with contextual shape descriptors. *International Journal of Computer Vision* 94(1):101–117.

Shechtman, E., and Irani, M. 2007. Matching local self-similarities across images and videos. In *Computer Vision and Pattern Recognition, 2007. CVPR'07. IEEE Conference on*, 1–8. IEEE.

Sun, Z.; Wang, C.; Zhang, L.; and Zhang, L. 2012. Query-adaptive shape topic mining for hand-drawn sketch recognition. In *Proceedings of the 20th ACM international conference on Multimedia*, 519–528. ACM.

Tropp, J. A. 2004. Greed is good: Algorithmic results for sparse approximation. *Information Theory, IEEE Transactions on* 50(10):2231–2242.

van Gemert, J. C.; Geusebroek, J.-M.; Veenman, C. J.; and Smeulders, A. W. 2008. Kernel codebooks for scene categorization. In *Computer Vision–ECCV 2008*. Springer. 696–709.

Yu, K.; Lin, Y.; and Lafferty, J. 2011. Learning image representations from the pixel level via hierarchical sparse coding. In *Computer Vision and Pattern Recognition (CVPR), 2011 IEEE Conference on*, 1713–1720. IEEE.